

Buckling analysis of nanocomposite cut out plate using domain decomposition method and orthogonal polynomials

M. Jamali ^{1a}, T. Shojaee ^{1b}, R. Kolahchi ^{*2}, and B. Mohammadi ^{1c}

¹ School of Mechanical Engineering, Iran University of Science and Technology, Tehran, Iran

² Faculty of Mechanical Engineering University of Kashan, Kashan, Iran

(Received June 21, 2016, Revised October 17, 2016, Accepted October 24, 2016)

Abstract. In this editorial, buckling analytical investigation of the nanocomposite plate with square cut out reinforced by carbon nanotubes (CNTs) surrounded by Pasternak foundation is considered. The plate is presumed has square cut out in center and resting on Pasternak foundation. CNTs are used as amplifier in plate for diverse distribution, such as uniform distribution (UD) and three patterns of functionally graded (FG) distribution types of CNTs (FG-X, FG-A and FG-O). Moreover, the effective mechanical properties of nanocomposite plate are calculated from the rule of mixture. Domain decomposition method and orthogonal polynomials are applied in order to define the shape function of nanocomposite plate with square cut out. Finally, Rayleigh-Ritz energy method is used to obtain critical buckling load of system. A detailed parametric study is conducted to explicit the effects of the dimensions of plate, length of square cut out, different distribution of CNTs, elastic medium and volume fraction of CNTs. It is found from results that increase the dimensions of plate and length of square cut out have negative impact on buckling behavior of system but considering CNTs in plate has positive influence.

Keywords: buckling analysis; nanocomposite plate; square cut out; domain decomposition method; orthogonal polynomials; Rayleigh-Ritz energy method

1. Introduction

Researchers in diverse scientific areas have founded that tiny scale materials can make powerful bond with around materials in comparison with great scale materials. Therefore, nanocomposites were produced; in such compound materials, amplifier is considered in nanoscale at least. Nowadays, nanocomposites are spreading swiftly; it is due to the fact that they have extraordinary properties. Nanocomposites are classified to four types with respect to their matrix such as, polymer matrix nanocomposites (PMNCs), ceramic matrix nanocomposites (CMNCs), metal matrix nanocomposites (MMNCs) and intermetallic matrix nanocomposites (IMNCs). PMNCs are more prominent in comparison with other types, because they have high strength, low weight, high electrical conductivity, high chemical resistance, etc (Sandler *et al.* 1999). Thus, this

*Corresponding author, Ph.D., E-mail: r.kolahchi@gmail.com

^a M.Sc. Student, E-mail: eng.mjamali@gmail.com

^b Ph.D., E-mail: ta_shojaee@cmeps2.iust.ac.ir

^c Ph.D., E-mail: bijan_mohammadi@iust.ac.i

kind of nanocomposites has wide application such as, car industry, aerospace, medical engineering, foodstuffs packaging, etc.

Buckling analysis of nanoplates has been considered by many researchers hitherto. Murmu and Pradhan (Murmu and Pradhan 2009) investigated the elastic buckling behavior of orthotropic small scale plates under biaxial compression. This study discussed the effects of the small scale on the buckling loads of nanoplates assuming various material and geometrical parameters. Buckling of single layer graphene sheet (SLGS) based on nonlocal elasticity and higher order shear deformation theory was addressed by Pradhan (2009). Bending, buckling and vibration analyses of nonhomogeneous nanotubes using generalized differential quadrature (GDQ) and nonlocal elasticity theory was presented by Pradhan and Phadikar (2009). Levy type solution method for vibration and buckling of nanoplates using nonlocal elasticity theory was reported by Aksencer and Aydogdu (2011). Results presented for different nonlocal parameter, different length of plates and different boundary conditions. In addition, results demonstrated that nonlocal effects for nanoscale plates should be considered. Hashemi and Samaei (2011) carried out the buckling analysis of micro/nanoscale plates via nonlocal elasticity theory. The effect of length scale on buckling behavior of a SLGS embedded in a Pasternak elastic medium using a nonlocal Mindlin plate theory was discussed by Samaei *et al.* (2011). It is understood that the nonlocal assumptions present larger buckling loads and stiffness of elastic medium in comparison with classical plate theory (CPT). Farajpour *et al.* (2011) reported buckling analysis of variable thickness nanoplates using nonlocal continuum mechanics. Result showed that the influence of percentage change of thickness on the stability of graphene sheets is more remarkable in the strip-type nanoplates (nanoribbons) than in the square-type nanoplates. Buckling response of orthotropic SLGS is investigated applying the nonlocal elasticity theory proposed by Farajpour *et al.* (2012). Differential quadrature method (DQM) has been applied to solve the governing equations for various boundary conditions. It is explicit that the nonlocal effects play a considerable role in the stability behavior of orthotropic nanoplates. Murmu *et al.* (2013) addressed nonlocal buckling of double-nanoplate-systems (DNPS) under biaxial compression. Both synchronous and asynchronous buckling phenomenon of biaxially compressed DNPS is presented in this work. Buckling analysis of double-orthotropic nanoplates embedded in Pasternak elastic medium using nonlocal elasticity theory was discussed by Radić *et al.* (2014). The influence of small scale coefficient, aspect ratio, and stiffness of internal elastic media and external elastic foundation, on the nondimensional buckling was considered. Golmakania and Rezatalab (2015) proposed the nonuniform biaxial buckling of orthotropic nanoplates embedded in an elastic medium based on nonlocal Mindlin plate theory. The effect of small scale effect, aspect ratio, polymer matrix properties, type of planar loading, mode numbers and boundary conditions were probed in details. Analytical solution for buckling of embedded laminated plates based on higher order shear deformation plate theory was addressed by Baseri *et al.* (2016).

CNTs can be used as amplifier in different structure (beam, plate, etc.) and produce nanocomposite system in order to enhance mechanical properties and improve behavior of system. Buckling analysis of laminated composite rectangular plates reinforced by CNTs using analytical and finite element methods was carried out by Ghorbanpour Arani *et al.* (2011). In this article, the effects of the CNTs orientation angle, the edge conditions, and the aspect ratio on the critical buckling load are considered using both the analytical and finite element methods. The critical buckling load of composite rectangle plate reinforced with CNTs subjected to axial compressive load using CPT is discussed by Jam and Maghamikia (Jam and Maghamikia 2011). Mohammadimehr *et al.* (2014a) proposed the buckling and vibration analysis of a double-bonded

nanocomposite piezoelectric plate reinforced by boron nitride nanotube based on the Eshelby-Mori-Tanaka approach applying modified couple stress theory under electro-thermo-mechanical loadings surrounded by an elastic foundation. The buckling analysis of annular composite plates reinforced by CNTs subjected to compressive and torsional loads was addressed by Asadi and Jam (2014). It is concluded that the stability of plate increases as the thickness or inner to outer ratio rises and when the CNTs arranged in the circumferential direction the highest buckling load is obtained. Mohammadimehr *et al.* (2014b) analyzed the biaxial buckling and bending of smart nanocomposite plate reinforced by CNTs using extended mixture rule approach. The effect of CNT waviness and aspect ratio on the buckling behavior of FG nanocomposite plates was investigated by Shams and Soltani (2015). Mosallaie Barzoki *et al.* (2015) presented the temperature-dependent nonlocal nonlinear buckling analysis of functionally graded SWCNT-reinforced microplates embedded in an orthotropic elastomeric medium. Bending, buckling and vibration responses of functionally graded carbon nanotube-reinforced composite beams were analyzed by Tagrara *et al.* (2015). Dynamic stability analysis of temperature-dependent FG-CNTR visco-plates resting on orthotropic elastomeric medium was presented by Kolahchi *et al.* (2016). The buckling behavior of laminated carbon nanotube reinforced composite (CNTRC) plates resting on Pasternak elastic foundations under in-plane loads was studied by Shams and Soltani (2016). The results presented that the geometric and mechanical properties and boundary conditions have prominent effects on the buckling behavior of laminated CNTRC plates.

With respect to the literature, no report has presented the buckling analysis of nanocomposite plate with square cut out. These considerations motivated us to present buckling analytical investigation of the nanocomposite plate with square cut out reinforced by CNTs embedded by Pasternak medium. Rule of mixture is used to obtain the mechanical properties of nanocomposite plate. This investigation will be made into the effect of the dimensions of plate, length of square cut out, different distribution of CNTs, elastic medium and volume fraction of CNTs.

The remainder of this essay is classified as follows: In Section 2, Eringen's nonlocal elasticity theory. In Section 3, the effective mechanical properties of nanocomposite plate are specified according to the rule of mixture. In Section 4, total energy of the system is obtained. In Section 5, at first by using domain decomposition method and orthogonal polynomials shape function of plate is determined, afterwards critical buckling load is distinguished by Rayleigh-Ritz method. In Section 6, numerical results of study are presented. In Section 7, conclusion of this dissertation is expressed.

2. Nonlocal elasticity theory

Consider a nanocomposite plate as illustrated in Fig. 1(a), with the length of a , width b and thickness h and a central square hole with length d . The plate is subjected to uniaxial load and surrounded by Pasternak foundation. Moreover, the plate is reinforced by CNTs in different distribution such as FG-UD, FG-X, FG-A and FG-O, in Fig. 1(b).

The local elasticity theory is applied in macro scale and this theory demonstrates that the stress state at any point depends on the strain state at this point; but, in nano/micro scale this hypothesis is not valid and some other theories are suggested such as Eringen's nonlocal elasticity theory. This theory expresses that the stress state at a reference point in the body is not related only to the strain state at this point but also on the strain states at all of the points throughout the body. According to this theory it can be express as (Ghorbanpour Arani *et al.* 2015)

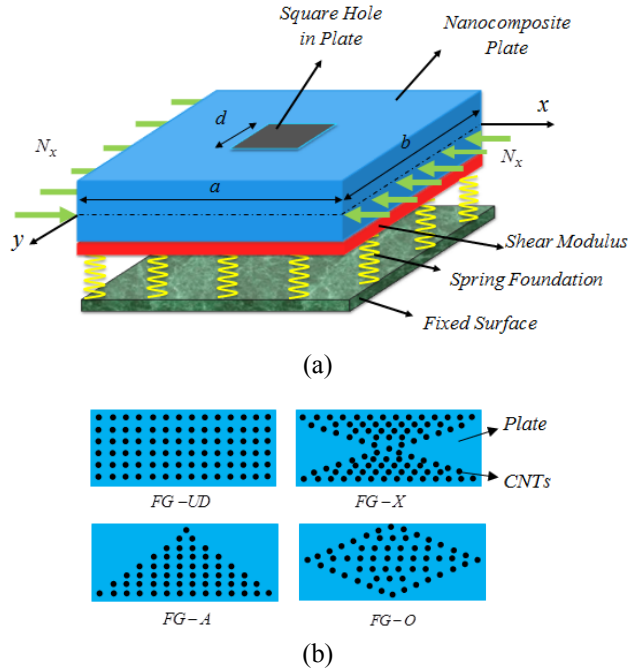


Fig. 1 (a) A nanocomposite cut out plate subjected to uniaxial buckling load surrounded by Pasternak foundation; (b) Distribution of CNTs in plate

$$\sigma_{ij}^{nl}(\mathbf{x}) = \int_V \alpha(|\mathbf{x} - \mathbf{x}'|, \tau) \sigma_{ij}^l dV(\mathbf{x}'), \quad \forall \mathbf{x} \in V \tag{1}$$

in which σ_{ij}^{nl} and σ_{ij}^l the nonlocal stress tensor and the local stress tensor, respectively. $\alpha(|\mathbf{x} - \mathbf{x}'|, \tau)$ demonstrates the nonlocal modulus, wherein $|\mathbf{x} - \mathbf{x}'|$ is the euclidean distance, and $\tau = e_0 a / l$ is a material constant that relates to the internal characteristic length a (e.g., distance between carbon-carbon bonds, granular size, lattice parameter) and external characteristic length l . The small scale parameter $e_0 a$ is gained from molecular dynamics, experimental results, experimental studies and molecular structure mechanics.

The constitutive equation of the nonlocal elasticity can be expressed as (Ghorbanpour Arani *et al.* 2015)

$$(1 - \mu^2 \nabla^2) \sigma_{ij}^{nl} = \sigma_{ij}^l, \tag{2}$$

where the parameter $\mu = (e_0 a)^2$ demonstrates the small scale effect regard to nanoscale, and ∇^2 is the Laplacian operator. It should be represented that the nonlocal stresses tensor change to a local one when the nonlocal parameter set to zero.

3. Mechanical properties of nanocomposite plate

In this study, orthotropic CNTs are applied in different shapes such as FG-UD, FG-X, FG-A and FG-O, to produce nanocomposite plate. The plate is assumed to be isotropic but after using

orthotropic CNTs in it, the system change to orthotropic structure. Therefore, by using CNTs in plate mechanical properties of system will be improved, thus, the effective mechanical properties of nanocomposite plate are extended through the rule of mixture and Young's modulus, E_{11} and E_{22} , and shear modulus, G_{12} , are (Ghorbanpour Arani *et al.* 2016a, b)

$$E_{11} = \eta_1 V_{CNT} E_{11}^{CNT} + V_m E^m, \tag{3}$$

$$\frac{\eta_2}{E_{22}} = \frac{V_{CNT}}{E_{22}^{CNT}} + \frac{V_m}{E^m}, \tag{4}$$

$$\frac{\eta_3}{G_{12}} = \frac{V_{CNT}}{G_{12}^{CNT}} + \frac{V_m}{G^m}, \tag{5}$$

in which $E_{11}^{CNT}, E_{22}^{CNT}$ and G_{12}^{CNT} are Young's modulus and shear modulus of CNTs, respectively and E^m, G^m show the corresponding properties related to matrix. The CNT efficiency parameters, η_j ($j = 1, 2, 3$), demonstrate the scale-dependent material properties obtained by matching the effective mechanical properties of nanocomposite plate calculated from the MD simulations with those from the rule of mixture. The relation between volume fractions of CNT, V_{CNT} , and volume fractions of matrix, V_m , expressed as (Ghorbanpour Arani *et al.* 2015)

$$V_{CNT} + V_m = 1. \tag{6}$$

The different shapes of the distributions of the CNTs along the thickness direction have been depicted in Fig. 1(b), are

$$UD: V_{CNT} + V_{CNT}^*, \tag{7}$$

$$FGA: V_{CNT} = \left(1 - \frac{2z}{h}\right) V_{CNT}^*, \tag{8}$$

$$FGO: V_{CNT} = 2 \left(1 - \frac{2|z|}{h}\right) V_{CNT}^*, \tag{9}$$

$$FGX: V_{CNT} = 2 \left(\frac{2|z|}{h}\right) V_{CNT}^*, \tag{10}$$

where

$$V_{CNT}^* = \frac{W_{CNT}}{W_{CNT} + \left(\frac{\rho_{CNT}}{\rho_m}\right) - \left(\frac{\rho_{CNT}}{\rho_m}\right) W_{CNT}}, \tag{11}$$

in which w_{CNT} expresses the mass fraction of nanotube. The Poisson's ratio, ν_{12} , of the nanocomposite plate is

$$\nu_{12} = V_{CNT}\nu_{12}^{CNT} + V_m\nu^m, \quad (12)$$

where ν_{12}^{CNT} and ν^m are Poisson's ratios of CNTs and plate, respectively.

The constitutive equations of the nonlocal elasticity are

$$\begin{Bmatrix} \sigma_{xx} \\ \sigma_{yy} \\ \sigma_{xy} \end{Bmatrix} = \begin{Bmatrix} C_{11} & C_{12} & 0 \\ C_{12} & C_{22} & 0 \\ 0 & 0 & C_{66} \end{Bmatrix} \begin{Bmatrix} \varepsilon_{xx} \\ \varepsilon_{yy} \\ \varepsilon_{xy} \end{Bmatrix}, \quad (13)$$

in which σ_{ij} and ε_{ij} are stress and strain, respectively. C_{ij} are elasticity coefficients and with respect to orthotropic structure, they are considered as (Wattanasakulpong and Chaikittiratana 2015)

$$C_{11} = \frac{E_{11}}{1-\nu_{12}\nu_{21}}, \quad C_{22} = \frac{E_{22}}{1-\nu_{12}\nu_{21}}, \quad C_{12} = \frac{\nu_{21}E_{11}}{1-\nu_{12}\nu_{21}}, \quad C_{66} = G_{12}. \quad (14)$$

4. Energy method

In order to governing equations of system, energy method is applied (Pan *et al.* 2013)

$$\Pi = U - W, \quad (15)$$

where, U and W are strain energy and external works, respectively and Π is total energy of system.

4.1 Strain energy

Strain energy can be obtained as (Ghorbanpour Arani *et al.* 2014)

$$U = \frac{1}{2} \int_A \int_{-\frac{h}{2}}^{\frac{h}{2}} (\sigma_{xx}\varepsilon_{xx} + \sigma_{yy}\varepsilon_{yy} + \sigma_{xy}\varepsilon_{xy}) dz dA. \quad (16)$$

By applying CPT, Refs. (Ashoori Movassagh and Mahmoodi 2013, Ghorbanpour Arani and Shokravi 2014) and Eq. (14) in Eq. (17)

$$U = \frac{1}{2} \int_A \left(-M_x \frac{\partial^2}{\partial x^2} w(x, y) - 2M_{xy} \frac{\partial^2}{\partial y \partial x} w(x, y) - M_y \frac{\partial^2}{\partial y^2} w(x, y) \right) dA \quad (17)$$

in which moment resultants are considered as (Reddy 2003)

$$(M_x, M_y, M_{xy}) = \int_{-\frac{h}{2}}^{\frac{h}{2}} (\sigma_x, \sigma_y, \sigma_{xy}) z dz, \quad (18)$$

4.2 External works

According to Fig. 1, the nanocomposite plate is subjected to two types of forces such as:

• **Foundation forces**

The plate is embedded by Pasternak foundation; as it is known, this foundation model is considers both normal (K_w) and shear (G_p) loads. Therefore, the work of this foundation can be obtained as (Ghorbanpour Arani *et al.* 2012)

$$W_e = -\int_A (K_w w - G_p \nabla^2 w) w dA, \tag{19}$$

• **Buckling load**

K_w and G_p are Winkler’s spring modulus and shear foundation parameters, respectively.

The nanocomposite plate is subjected to buckling, thus the work of this force can be calculated as (Pan *et al.* 2013)

$$W_b = -\frac{1}{2} \int_A \left(N_{xx} \left(\frac{\partial}{\partial x} w(x, y) \right)^2 + N_{yy} \left(\frac{\partial}{\partial y} w(x, y) \right)^2 \right) dA, \tag{20}$$

the buckling load is uniaxial, so $N_{xx} = -P$ and $N_{yy} = 0$.

With respect to Eringen’s nonlocal elasticity theory and energy method, total energy of nanocomposite plate is equal to

$$\Pi = \int_A \left(\begin{aligned} &\mu^2 P \left(\frac{\partial^2}{\partial x^2} \right)^2 + \mu^2 P \left(\frac{\partial^2 w}{\partial y \partial x} \right)^2 - \frac{1}{2} P \left(\frac{\partial w}{\partial x} \right)^2 + \mu^2 P \left(\frac{\partial w}{\partial x} \right) \left(\frac{\partial^3 w}{\partial x^3} \right) + \mu^2 P \left(\frac{\partial w}{\partial x} \right) \left(\frac{\partial^3 w}{\partial y^2 \partial x} \right) \\ &- 2\mu^2 K_w w \left(\frac{\partial^2 w}{\partial x^2} \right) + 2\mu^2 \left(\frac{\partial w}{\partial x} \right) G_p \left(\frac{\partial^3 w}{\partial x^3} \right) + \mu^2 G_p w \left(\frac{\partial^4 w}{\partial x^4} \right) + 2\mu^2 \left(\frac{\partial^2}{\partial x^2} \right) G_p \left(\frac{\partial^2}{\partial y^2} \right) \\ &+ 2\mu^2 \left(\frac{\partial w}{\partial x} \right) G_p \left(\frac{\partial^3 w}{\partial x^3} \right) + 2\mu^2 G_p w \left(\frac{\partial^4 w}{\partial y^2 \partial x^2} \right) - 2\mu^2 K_w w \left(\frac{\partial^2 w}{\partial y^2} \right) + \mu^2 w G_p \left(\frac{\partial^4 w}{\partial y^4} \right) \\ &+ 2\mu^2 \left(\frac{\partial w}{\partial x} \right) G_p \left(\frac{\partial^3 w}{\partial y^2 \partial x} \right) + 2\mu^2 \left(\frac{\partial w}{\partial x} \right) G_p \left(\frac{\partial^3 w}{\partial y^3} \right) + \mu^2 \left(\frac{\partial^2 w}{\partial y^2} \right)^2 G_p - w G_p \left(\frac{\partial^2 w}{\partial x^2} \right) \\ &- w G_p \left(\frac{\partial^2 w}{\partial y^2} \right) - M_{xy} \left(\frac{\partial^2 w}{\partial y \partial x} \right) - \frac{1}{2} M_y \left(\frac{\partial^2 w}{\partial y^2} \right) \end{aligned} \right) dA, \tag{21}$$

where

$$M_x = -D_{11} \left(\frac{\partial^2}{\partial x^2} w(x, y) \right) h - D_{12} \left(\frac{\partial^2}{\partial x^2} w(x, y) \right) h, \tag{22}$$

$$M_y = -D_{12} \left(\frac{\partial^2}{\partial x^2} w(x, y) \right) h - D_{22} \left(\frac{\partial^2}{\partial y^2} w(x, y) \right) h, \tag{23}$$

$$M_{xy} = -2D_{66} \left(\frac{\partial^2}{\partial y \partial x} w(x, y) \right) h, \tag{24}$$

and the stiffness components in aforementioned equations can be specified as (Ghorbanpour Arani *et al.* 2016b)

$$(D_{11}, D_{22}, D_{12}, D_{66}) = \int_{-\frac{h}{2}}^{\frac{h}{2}} z^2 \cdot (C_{11}(z), C_{22}(z), C_{12}(z), C_{66}(z)) dz, \quad (25)$$

5. Buckling of nanocomposite plate with central square cut out

5.1 Domain decomposition method and orthogonal polynomials

In this section, the shape function of plate with central cut out in simply supported boundary conditions (S-S-S-S), will be calculated by applying domain decomposition method and orthogonal polynomials. At first domain decomposition method (Bhat 1985, Lam *et al.* 1989, Lam

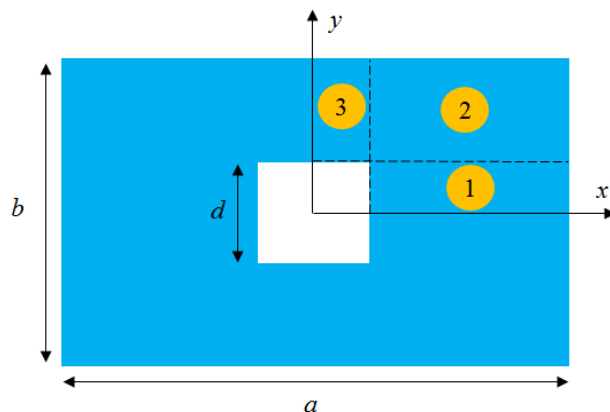


Fig. 2 Illustration of dividing the nanocomposite cut out plate to three sub-domains

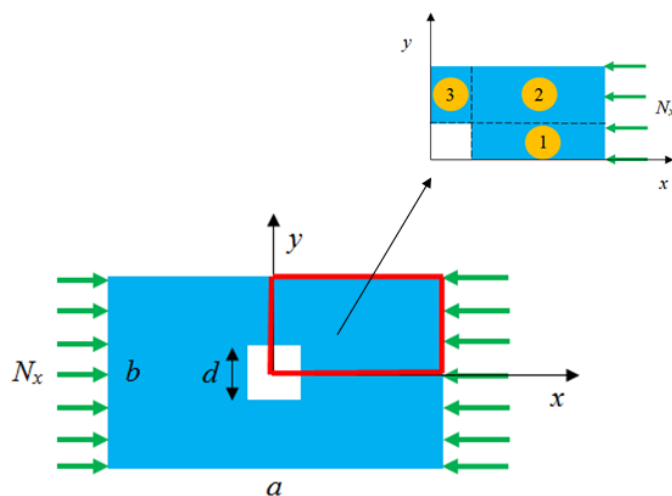


Fig. 3 A schematic of one fourth of plate divided to three sub-domains

and Hung 1990a, b, Liew *et al.* 1993, 1995, 2001, 2003, Pan *et al.* 2013), which considers not only the outer boundary conditions (S-S-S-S), but also the inner (cut out edges) free boundary condition, is used to divide plate to some sub-domain.

Because of the two symmetrical conditions only one quarter of the rectangular plate with a central square cut out need to be considered as Fig. 2, therefore, one fourth of plate is divided to three sub-domains as Fig. 3.

After partitioning nanocomposite plate with a central square cut out, shape function should be determined. Orthogonal polynomials (Bhat 1985) are applied to present the shape function of each sub-domain which considers the geometric boundary conditions. The deflection shape functions for each sub-domain can be defined as

$$w^{(1)}(x, y) = \sum_{m=1}^M \sum_{n=1}^N A_{mn}^{(1)} f_m^{(1)}(x) g_n^{(1)}(y), \tag{26}$$

$$w^{(2)}(x, y) = \sum_{m=1}^M \sum_{n=1}^N A_{mn}^{(2)} f_m^{(2)}(x) g_n^{(2)}(y), \tag{27}$$

Table 1 Starting polynomials for sets of orthogonal polynomials (Pan *et al.* 2013)

Boundary conditions	Starting polynomials, $f_1(x)$	Generating functions, $g_0(x)$
Free-free		
$f_1''(0) = f_1'''(0) = 0,$ $f_1''(1) = f_1'''(1) = 0,$	1.0	x
Free-simply supported		
$f_1''(0) = f_1'''(0) = 0,$ $f_1''(1) = f_1'''(1) = 0,$	$1 - x$	$x^2 - 2x$
Free-clamped		
$f_1''(0) = f_1'''(0) = 0,$ $f_1''(1) = f_1'''(1) = 0,$	$3 - 4x + x^4$	x
Symmetric-free		
$f_1''(0) = f_1'''(0) = 0,$ $f_1''(1) = f_1'''(1) = 0,$	$1 + x^2$	$1 + x^2$
Symmetric-simply supported		
$f_1''(0) = f_1'''(0) = 0,$ $f_1''(1) = f_1'''(1) = 0,$	$5 - 6x^2 + x^4$	x^2
Symmetric-clamped		
$f_1''(0) = f_1'''(0) = 0,$ $f_1''(1) = f_1'''(1) = 0,$	$1 - 2x^2 + x^4$	$1 - x^2$
Anti-symmetric-simply supported		
$f_1''(0) = f_1'''(0) = 0,$ $f_1''(1) = f_1'''(1) = 0,$	$x - 2x^3 + x^4$	x^2

$$w^{(3)}(x, y) = \sum_{m=1}^M \sum_{n=1}^N A_{mn}^{(3)} f_m^{(3)}(x) g_n^{(3)}(y), \quad (28)$$

where, the superscripts (1), (2) and (3) are imply to sub-domain 1, 2 and 3 respectively. $w^{(i)}$ ($i = 1, 2, 3$) are the shape functions of sub-domain 1, 2 and 3 respectively. $A_{mn}^{(i)}$ are the undetermined coefficients of the shape functions $w^{(i)}$. $f_m^{(i)}(x)$ are polynomial functions which consider the essential boundary conditions along x -direction, while $g_n^{(i)}(y)$ are polynomial functions which consider the essential boundary conditions along y -direction. The orthogonal polynomial functions $f_m^{(i)}(x)$ and $g_n^{(i)}(y)$ are made by the Gram–Schmidt process (Bhat 1985), applying the initial polynomials ($f_1(x)$, $g_0(x)$) which initially satisfy the essential boundary conditions, can be calculated for different boundary conditions according to Table 1.

The process is as (Bhat 1985)

$$f_2(x) = (g_0(x) - A_1) f_1(x), \quad (29)$$

$$f_{k+1}(x) = (g_0(x) - A_k) f_k(x) - B_k f_{k-1}(x), \quad k \geq 2 \quad (30)$$

In order to specify functions $g_n(y)$ the same process of determining $f_m(x)$ as defined in Eqs. (29)-(32) can be used.

Therefore, shape functions of three sub-domains were defined hitherto and the final step in order to calculate buckling load, is to determine deflection functions of three sub-domains in terms of the undetermined coefficients of one the sub-domains. Thus, the best way is to apply some spots in the interconnecting boundary between sub-domains and according to the mathematical derivation, the undetermined coefficients of sub-domains 1, 2 and 3 are related together (Bhat 1985, Lam and Hung 1990a, b, Liew *et al.* 2001, 2003).

5.2 Rayleigh-Ritz method

Rayleigh-Ritz method is used to calculate buckling load of nanocomposite plate with a central square cut out. As noted before, because of the two symmetrical conditions only one quarter of the rectangular plate with a central square cut out need to be considered. The total energy of cut out plate is determined as

$$\Pi = \Pi^{(1)} + \Pi^{(2)} + \Pi^{(3)}, \quad (31)$$

$\Pi^{(i)}$ ($i = 1, 2, 3$) are total energy of sub-domains 1, 2 and 3, respectively and they are presented in Appendix A. Therefore, total energy of cut out plate is specified in terms of the undetermined coefficients of shape function of sub-domain 1. The critical buckling load of the cut out plate after applying Rayleigh-Ritz method is determined by putting the coefficient determinant of the equations equal to zero.

6. Results and discussion

In this section, the results of considering buckling analysis in nanocomposite plate with square cut out reinforced by CNTs resting on Pasternak foundation are presented through some figures. The goal of this essay is to distinguish the effects of the dimensions of plate, length of square cut

Table 2 Material properties of matrix and CNTs (Shams and Soltani 2016)

Matrix	CNTs
$E^m = 2.1$ (GPa)	$E_{11}^{CNT} = 5.6466$ (TPa)
$\nu_m = 0.34$	$E_{22}^{CNT} = 7.08$ (TPa)
	$G_{12}^{CNT} = 1.9447$ (TPa)
	$\nu_{12}^{CNT} = 0.175$ (TPa)

Table 3 A comparison between the buckling analysis of SLGS using the theories of classical plate, higher order shear deformation and Mindlin plate

a/h	e_0a	CPT (Pradhan and Murmu 2009)	Higher order plate theory (Pradhan 2009)	Mindlin plate theory (Hashemi and Samaei 2011)	Present
100	0.0	9.8791	9.8671	9.8671	9.8790
	0.5	9.4156	9.4031	9.4029	9.4156
	1.0	8.9947	8.9807	8.9803	8.9945
	1.5	8.6073	8.5947	8.5939	8.6073
	2.	8.2537	8.2405	8.2393	8.2533
20	0.0	9.8177	9.8067	9.8067	9.8172
	0.5	9.3570	9.3455	9.3455	9.3570
	1.0	8.9652	8.9528	8.9527	8.9648
	1.5	8.5546	8.5420	8.5420	8.5546
	2.0	8.2114	8.1900	8.1898	8.2111

Table 4 A comparison by considering CNTs for different (K_w, G_p) and V_{CNT}^*

V_{CNT}^*	(K_w, G_p)					
	(0,0)		(1000,0)		(1000,10)	
	(Shams and Soltani 2016)	Present	(Shams and Soltani 2016)	Present	(Shams and Soltani 2016)	Present
0.11	31.1573	31.1663	40.7179	40.7280	59.5620	59.5715
0.14	37.3815	37.3923	46.9422	46.9511	65.7863	65.7013
0.17	48.2092	48.2202	57.7699	57.7814	76.6144	76.6261

out, different distribution of CNTs (FG-X, FG-UD, FG-A and FG-O), elastic medium and volume fraction of CNTs on critical buckling load of plate. Here Poly-co-vinylene, referred to as PmPV, and orthotropic CNTs are selected as the matrix and the reinforcement materials, respectively. The geometrical parameters of structure are assumed as, $a = b = 30$ nm, $d = 0.1 \times b$ and $h = 1$ nm; in addition, the material properties of CNTs and PmPV are presented in Table 2.

In order to validate the result of this study with other article, a comparison among the buckling analysis of CPT (Pradhan and Murmu 2009), higher order plate theory (Pradhan 2009), Mindlin plate theory (Hashemi and Samaei 2011) and present essay is reported in Table 3.

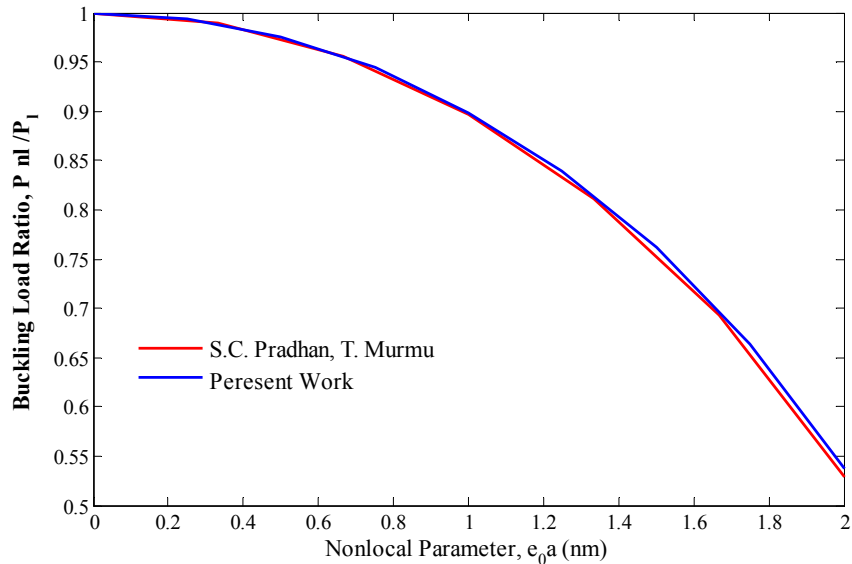


Fig. 4 Comparison of buckling load ratio versus nonlocal parameter

In this table, critical buckling load for diverse values of nonlocal parameter and aspect ratio of length to thickness is defined. As can be seen, the present results closely match with those presented by Hashemi and Samaei (2011), Pradhan and Murmu (2009) and Pradhan (2009). Moreover, a comparison of buckling load ratio with respect to nonlocal parameter between Pradhan and Murmu (2009) and present study is provided in Fig. 4.

To compare the results of this article by considering CNTs as booster, Table 4 shows a comparison between Shams and Soltani (2016) and present study.

In this editorial, buckling load ratio, dimensionless Winkler modulus and shear modulus are specified as follows

$$\text{Buckling load ratio} = \frac{\text{Buckling load from nonlocal theory } (P_{nl})}{\text{Buckling load from local theory } (P_l)}, \quad (32)$$

$$K_w = \frac{K_w h}{E^m}, \quad (33)$$

$$G_p = \frac{G_p}{h E^m}. \quad (34)$$

It is noted, figures presented in this section are depicted according to UD distribution.

Fig. 5 illustrates the effect of length of plate on buckling load ratio by considering dimensionless nonlocal parameter. As can be seen, by increasing nonlocal parameter, critical buckling load ratio decreases. The figure shows that increase length causes more buckling load ratio, because by increasing length, stiffness of system decreases so the critical buckling load decreases too but variation of local buckling load is more than nonlocal buckling load, therefore, the critical buckling load ratio increases. It is apparent that the effect of length on the buckling load ratio is more remarkable in high value of nonlocal parameter.

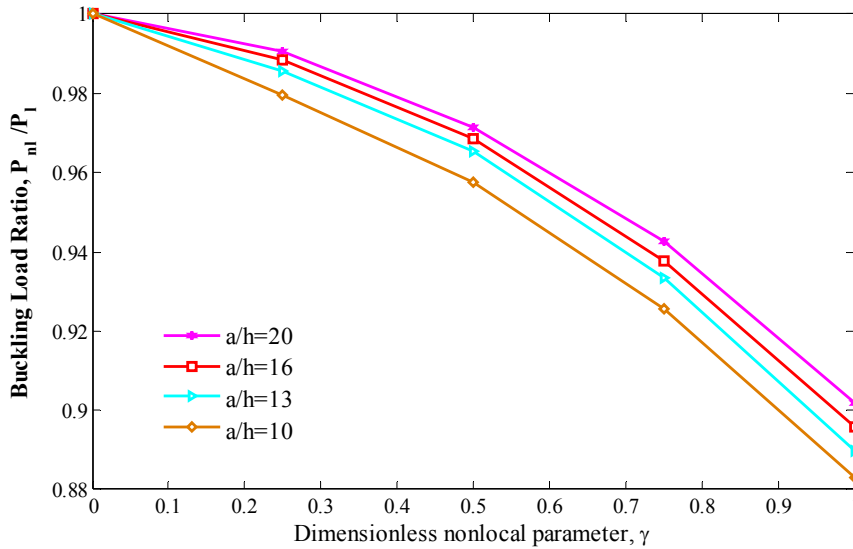


Fig. 5 Effect of the length of plate on critical buckling load ratio in terms of the dimensionless nonlocal parameter

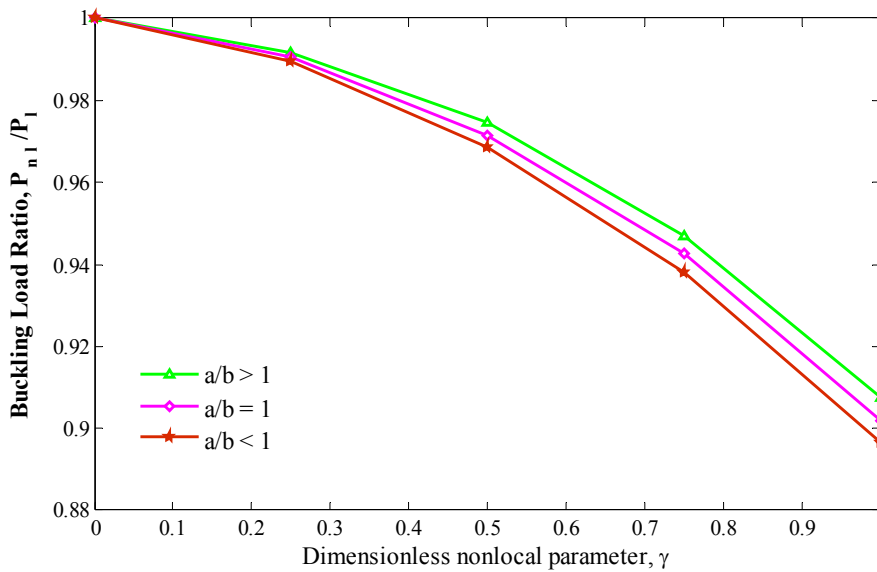


Fig. 6 Effect of the aspect ratio of plate on buckling load ratio versus the dimensionless nonlocal parameter

Variation of critical buckling load ratio in terms of nonlocal parameter with respect to different aspect ratio of nanocomposite square cut out plate is analyzed in Fig. 6. It is obvious that the effectiveness order of aspect ratio on buckling load ratio from high to low is as $a/b > 1$, $a/b = 1$ and $a/b < 1$, respectively. To understand the reason of this order, it is better to look at Fig. 1 and consider the length and width of plate and the direction of uniaxial buckling load. Moreover, by keep in view to the trend of figure, buckling load ratio decreases by increasing nonlocal parameter.

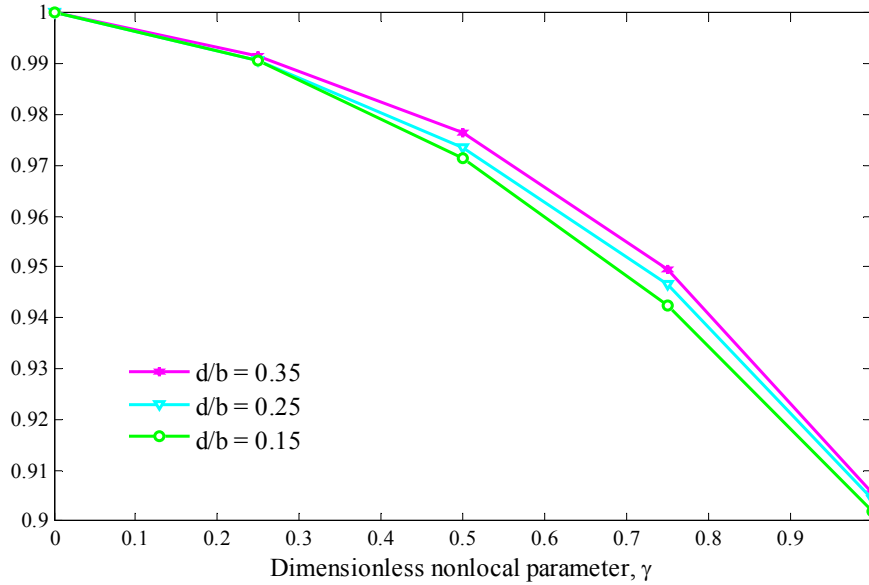


Fig. 7 Variation of the critical buckling load ratio by considering dimensionless nonlocal parameter for different length of square cut out in plate

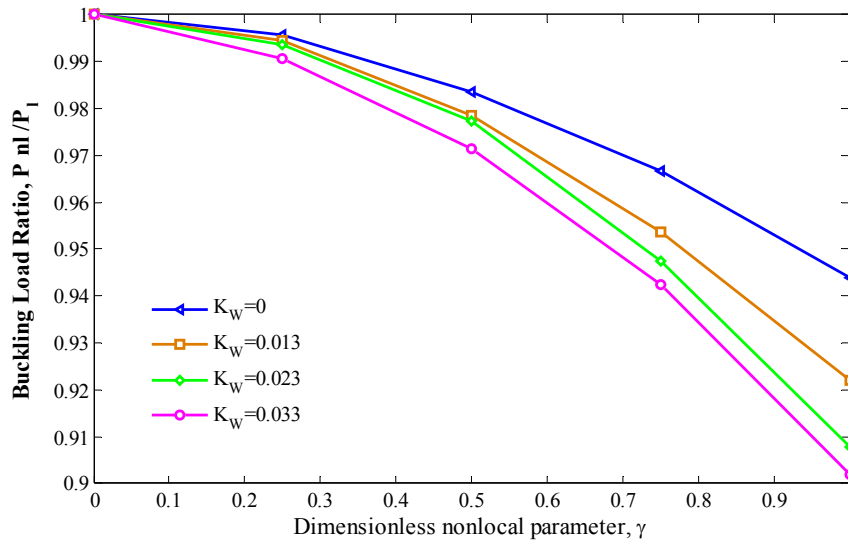


Fig. 8 Buckling load ratio versus dimensionless nonlocal parameter for different values of Winkler modulus parameter

Fig. 7 considers the effect of length of square cut out in nanocomposite plate on buckling load ratio in terms of the nonlocal parameter. It is apparent, existence a hole in plate causes defect in system and weaken the buckling behavior, therefore, by increasing length of square cut out in plate buckling load ratio increase. In addition, the effect of length of hole on critical buckling load ratio is more considerable for high dimensionless nonlocal parameter.

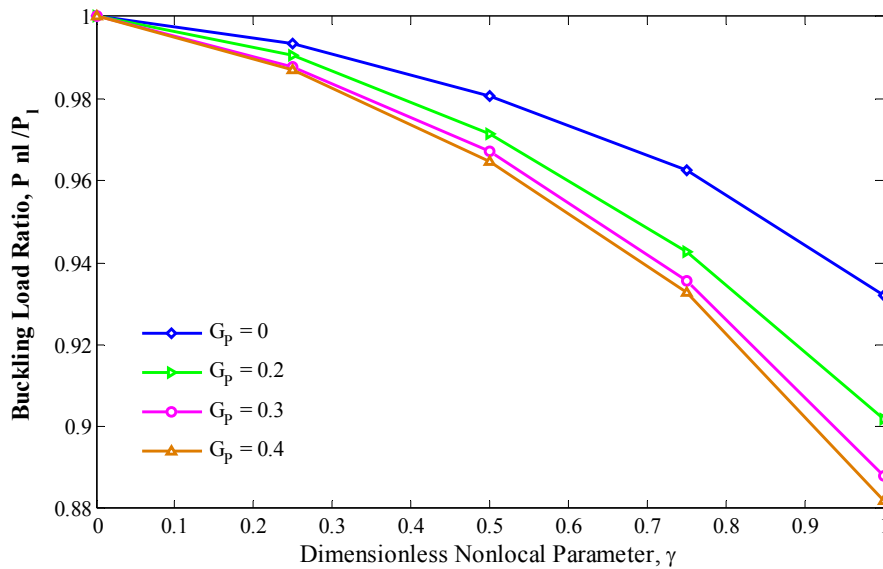


Fig. 9 Buckling load ratio versus dimensionless nonlocal parameter for different shear modulus parameter

Now the effect of the elastic medium on critical buckling ratio is examined in this section. Figs. 8 and 9 analyze the variation of buckling load ratio by considering nonlocal parameter keep in view different magnitude of Winkler modulus parameter (K_w) and shear modulus parameter (G_p). It is obvious that considering Winkler modulus parameter and shear modulus parameter, improve the buckling behavior of plate, because Winkler foundation imposes normal force and Pasternak medium impose normal and shear forces to system, therefore, considering these foundation increase the stiffness of system and buckling load ratio. Keep in view above-mentioned and the trend of Figs. 8 and 9, the effect of Pasternak foundation is more than Winkler foundation.

In this study, in order to improve the mechanical properties of system, CNTs are used as amplifier. One of the important factors of CNTs distribution is their volume fraction; therefore, Fig. 10 demonstrates variation of buckling ratio in terms of nonlocal parameter by considering different volume fraction for different efficiency parameters as follow (Zhu *et al.* 2012)

$$V_{CNT}^* = 0.11: \quad \eta_1 = 0.149, \quad \eta_2 = \eta_3 = 0.934 \tag{35}$$

$$V_{CNT}^* = 0.14: \quad \eta_1 = 0.150, \quad \eta_2 = \eta_3 = 0.941 \tag{36}$$

$$V_{CNT}^* = 0.17: \quad \eta_1 = 0.149, \quad \eta_2 = \eta_3 = 1.381 \tag{37}$$

It is explicit that increase volume fraction causes more critical buckling load, because volume fraction is a symbol of CNTs numbers in plate, thus, increase volume fraction leads to more CNTs in plate and improve mechanical properties of system.

As mentioned before, CNTs are used as amplifier in four different shapes such as FG-UD, FG-X, FG-A and FG-O. Fig. 11 shows the effect of different distribution of CNTs in plate on buckling load ratio with respect to nonlocal parameter. It is distinct that Isotropic type (plate without CNTs)

has minimum effect on critical buckling load ratio in comparison with other types which types have CNTs in plate. Moreover, FG-X has more effect on improvement behavior of nanocomposite cut out plate in comparison with FG-UD, FG-A and FG-O. The reason is that the stiffness of system changes with the form of CNT distribution in matrix. However, it can be comprehend that CNTs distribution close to top and bottom are more efficient than those distributed nearby the mid-plane for increasing the stiffness of plates.

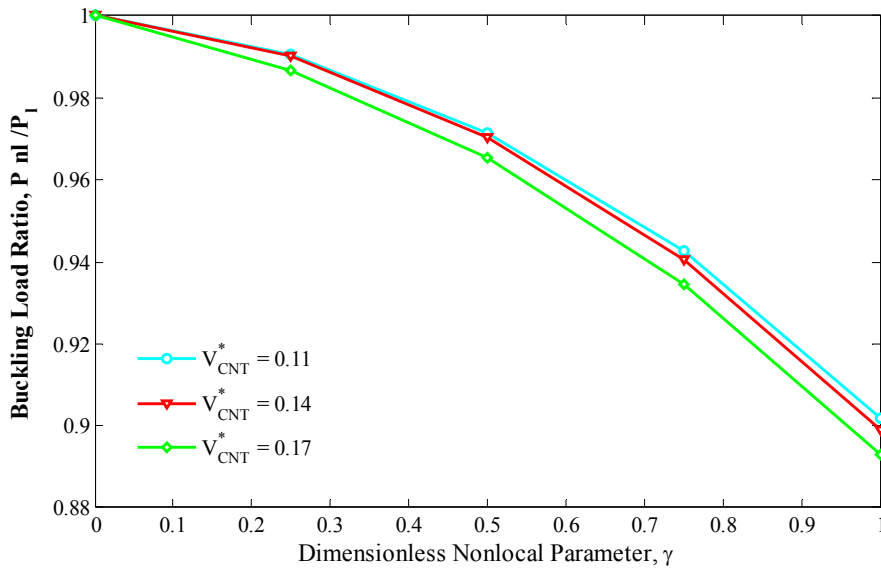


Fig. 10 Variation of the critical buckling load ratio in terms of dimensionless nonlocal parameter for different CNTs volume fraction

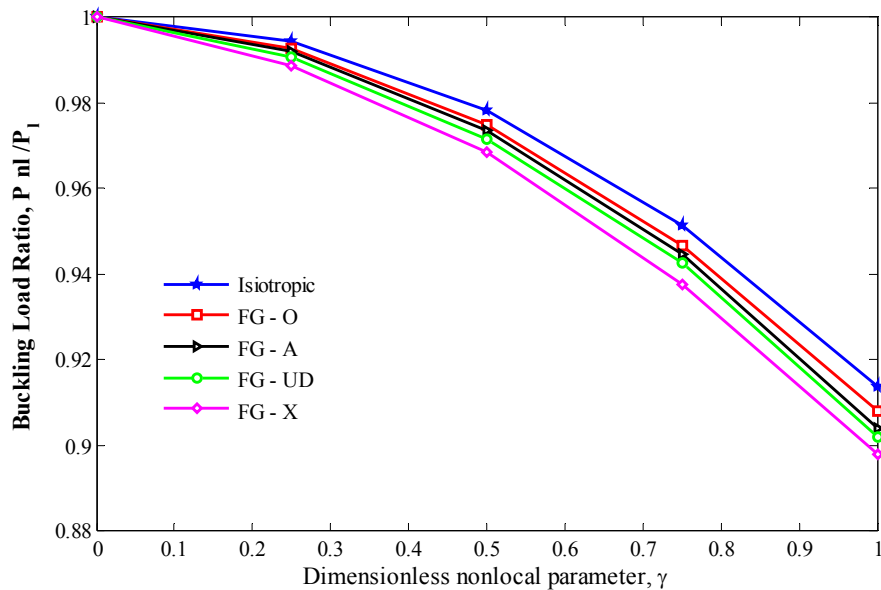


Fig. 11 Effect of the distribution of CNTs on buckling load ratio versus dimensionless nonlocal parameter

7. Conclusions

In this dissertation, buckling analysis of nanocomposite plate with square cut out reinforced by CNTs was investigated. The plate was surrounded by Pasternak foundation and reinforced by CNTs in different FG distributions (FG-X, FG-UD, FG-A and FG-O). Role of mixture was applied to determine the effective mechanical properties of nanocomposite plate and Eringen's nonlocal elasticity theory was used to consider nanoscale effect. In order to define the shape function of nanocomposite plate with square cut out, domain decomposition method and orthogonal polynomials were applied. Finally, Rayleigh-Ritz energy method was used to obtain critical buckling load of system so that the impact of the dimensions of plate, length of square cut out, different distribution of CNTs, elastic medium and volume fraction of CNTs on critical buckling load were distinguished. Results demonstrated that:

- By increasing dimensions of plate the buckling load ratio of nanocomposite plate with square cut out rises.
- Existence a hole in plate causes defect in system and weaken the buckling behavior, therefore, by increasing length of square cut out in plate buckling load ratio increase.
- The effect of different parameters on buckling load ratio is more remarkable in high value of nonlocal parameter.
- Increase volume fraction of CNTs causes more critical buckling load.
- By considering CNTs in plate, critical buckling load increases.
- FG-X has more effect on improvement behavior of nanocomposite plate in comparison with FG-UD, FG-A and FG-O.

The results provided in this paper would be useful in design and manufacturing of composite systems especially in nano/micro-mechanical systems.

References

- Aksencer, T. and Aydogdu, M. (2011), "Levy type solution method for vibration and buckling of nanoplates using nonlocal elasticity theory", *Physica E: Low-dimensional Systems and Nanostructures*, **43**(4), 954-959.
- Asadi, E. and Jam, J.E. (2014), "Analytical and numerical buckling analysis of carbon nanotube reinforced annular composite plates", *Int. J. Adv. Des. Manuf. Technol.*, **7**(2), 35-44.
- Ashoori Movassagh, A. and Mahmoodi, M.J. (2013), "A micro-scale modeling of Kirchhoff plate based on modified strain-gradient elasticity theory", *Eur. J. Mech. - A/Solids*, **40**, 50-59.
- Baseri, V., Soleimani Jafari, G. and Kolahchi, R. (2016), "Analytical solution for buckling of embedded laminated plates based on higher order shear deformation plate theory", *Steel Compos. Struct., Int. J.*, **21**(4), 883-919.
- Bhat, R.B. (1985), "Natural frequencies of rectangular plates using characteristic orthogonal polynomials in rayleigh-ritz method", *J. Sound Vib.*, **102**(4), 493-499.
- Farajpour, A., Danesh, M. and Mohammadi, M. (2011), "Buckling analysis of variable thickness nanoplates using nonlocal continuum mechanics", *Physica E: Low-dimensional Systems and Nanostructures*, **44**(3), 719-727.
- Farajpour, A., Shahidi, A.R., Mohammadi, M. and Mahzoon, M. (2012), "Buckling of orthotropic micro/nanoscale plates under linearly varying in-plane load via nonlocal continuum mechanics", *Compos. Struct.*, **94**(5), 1605-1615.
- Ghorbanpour Arani, A. and Shokravi, M. (2014), "Vibration response of visco-elastically coupled double-

- layered visco-elastic graphene sheet systems subjected to magnetic field via strain gradient theory considering surface stress effects”, *Proceedings of the Institution of Mechanical Engineers, Part N: Journal of Nanoengineering and Nanosystems*, **229**(4), 180-190.
- Ghorbanpour Arani, A.G., Maghamikia, S., Mohammadimehr, M. and Arefmanesh, A. (2011), “Buckling analysis of laminated composite rectangular plates reinforced by SWCNTs using analytical and finite element methods”, *J. Mech. Sci. Technol.*, **25**(3), 809-820.
- Ghorbanpour Arani, A., Kolahchi, R. and Vossough, H. (2012), “Buckling analysis and smart control of SLGS using elastically coupled PVDF nanoplate based on the nonlocal Mindlin plate theory”, *Physica B: Condensed Matter*, **407**(22), 4458-4465.
- Ghorbanpour Arani, A., Kolahchi, R., Mosayyebi, M. and Jamali, M. (2014), “Pulsating fluid induced dynamic instability of visco-double-walled carbon nano-tubes based on sinusoidal strain gradient theory using DQM and Bolotin method”, *Int. J. Mech. Mater. Des.*, **12**(1), 17-38.
- Ghorbanpour Arani, A., Jamali, M., Mosayyebi, M. and Kolahchi, R. (2015), “Analytical modeling of wave propagation in viscoelastic functionally graded carbon nanotubes reinforced piezoelectric microplate under electro-magnetic field”, *Proceedings of the Institution of Mechanical Engineers, Part N: Journal of Nanoengineering and Nanosystems*. [In press]
- Ghorbanpour Arani, A., Jamali, M., Ghorbanpour-Arani, A., Kolahchi, R. and Mosayyebi, M. (2016a), “Electro-magneto wave propagation analysis of viscoelastic sandwich nanoplates considering surface effects”, *Proceedings of the Institution of Mechanical Engineers, Part C: Journal of Mechanical Engineering Science*. [In press]
- Ghorbanpour Arani, A., Jamali, M., Mosayyebi, M. and Kolahchi, R. (2016b), “Wave propagation in FG-CNT-reinforced piezoelectric composite micro plates using viscoelastic quasi-3D sinusoidal shear deformation theory”, *Composites Part B: Engineering*, **95**, 209-224.
- Golmakani, M.E. and Rezatalab, J. (2015), “Nonuniform biaxial buckling of orthotropic nanoplates embedded in an elastic medium based on nonlocal Mindlin plate theory”, *Composite Structures*, **119**, 238-250.
- Hashemi, S.H. and Samaei, A.T. (2011), “Buckling analysis of micro/nanoscale plates via nonlocal elasticity theory”, *Physica E: Low-dimensional Systems and Nanostructures*, **43**(7), 1400-1404.
- Jam, J.E. and Maghamikia, S. (2011), “Elastic buckling of composite plate reinforced with carbon nano tubes”, *Int. J. Eng. Sci. Technol.*, **3**, 4090-4101.
- Kolahchi, R., Safari, M. and Esmailpour, M. (2016), “Dynamic stability analysis of temperature-dependent functionally graded CNT-reinforced visco-plates resting on orthotropic elastomeric medium”, *Compos. Struct.*, **150**, 255-265.
- Lam, K.Y. and Hung, K.C. (1990a), “Orthogonal polynomials and sub-sectioning method for vibration of plates”, *Comput. Struct.*, **34**(6), 827-834.
- Lam, K.Y. and Hung, K.C. (1990b), “Vibration study on plates with stiffened openings using orthogonal polynomials and partitioning method”, *Comput. Struct.*, **37**(3), 295-301.
- Lam, K.Y., Hung, K.C. and Chow, S.T. (1989), “Vibration analysis of plates with cutouts by the modified Rayleigh-Ritz method”, *Appl. Acoust.*, **28**(1), 49-60.
- Liew, K.M., Hung, K.C. and Lim, M.K. (1993), “Method of domain decomposition in vibrations of mixed edge anisotropic plates”, *Int. J. Solid. Struct.*, **30**(23), 3281-3301.
- Liew, K.M., Hung, K.C. and Sum, Y.K. (1995), “Flexural vibration of polygonal plates: treatments of sharp re-entrant corners”, *J. Sound Vib.*, **183**(2), 221-238.
- Liew, K.M., Ng, T.Y. and Kitipornchai, S. (2001), “A semi-analytical solution for vibration of rectangular plates with abrupt thickness variation”, *Int. J. Solid. Struct.*, **38**(28-29), 4937-4954.
- Liew, K.M., Kitipornchai, S., Leung, A.Y.T. and Lim, C.W. (2003), “Analysis of the free vibration of rectangular plates with central cut-outs using the discrete Ritz method”, *Int. J. Mech. Sci.*, **45**(5), 941-959.
- Mohammadimehr, M., Mohandes, M. and Moradi, M. (2014a), “Size dependent effect on the buckling and vibration analysis of double-bonded nanocomposite piezoelectric plate reinforced by boron nitride nanotube based on modified couple stress theory”, *J. Vib. Control*, **22**(7), 1790-1807.
- Mohammadimehr, M., Roustavi, B. and Ghorbanpour-Arani, A. (2014b), “Biaxial Buckling and Bending

- of Smart Nanocomposite Plate Reinforced by CNTs using Extended Mixture Rule Approach”, *Mech. Adv. Compos. Struct.*, **1**(1), 17-26.
- Mosallaie Barzoki, A.A., Loghman, A. and Ghorbanpour Arani, A. (2015), “Temperature-dependent nonlocal nonlinear buckling analysis of functionally graded SWCNT-reinforced microplates embedded in an orthotropic elastomeric medium”, *Struct. Eng. Mech., Int. J.*, **53**(3), 479-517.
- Murmu, T. and Pradhan, S.C. (2009), “Buckling of biaxially compressed orthotropic plates at small scales”, *Mech. Res. Commun.*, **36**(8), 933-938.
- Murmu, T., Sienz, J., Adhikari, S. and Arnold, C. (2013), “Nonlocal buckling of double-nanoplate-systems under biaxial compression”, *Compos. Part B: Eng.*, **44**(1), 84-94.
- Pan, Z., Cheng, Y. and Liu, J. (2013), “A semi-analytical analysis of the elastic buckling of cracked thin plates under axial compression using actual non-uniform stress distribution”, *Thin-Wall. Struct.*, **73**, 229-241.
- Pradhan, S.C. (2009), “Buckling of single layer graphene sheet based on nonlocal elasticity and higher order shear deformation theory”, *Physics Letters A*, **373**(45), 4182-4188.
- Pradhan, S.C. and Murmu, T. (2009), “Small scale effect on the buckling of single-layered graphene sheets under biaxial compression via nonlocal continuum mechanics”, *Computat. Mater. Sci.*, **47**(1), 268-274.
- Pradhan, S.C. and Phadikar, J.K. (2009), “Bending, buckling and vibration analyses of nonhomogeneous nanotubes using GDQ and nonlocal elasticity theory”, *Struct. Eng. Mech., Int. J.*, **33**(2), 193-213.
- Radić, N., Jeremić, D., Trifković, S. and Milutinović, M. (2014), “Buckling analysis of double-orthotropic nanoplates embedded in Pasternak elastic medium using nonlocal elasticity theory”, *Compos. Part B: Eng.*, **61**, 162-171.
- Reddy, J.N. (2003), *Mechanics of Laminated Composite Plates and Shells: Theory and Analysis*, CRC Press.
- Samaei, A.T., Abbasion, S. and Mirsayar, M.M. (2011), “Buckling analysis of a single-layer graphene sheet embedded in an elastic medium based on nonlocal Mindlin plate theory”, *Mech. Res. Commun.*, **38**(7), 481-485.
- Sandler, J., Shaffer, M.S.P., Prasse, T., Bauhofer, W., Schulte, K. and Windle, A.H. (1999), “Development of a dispersion process for carbon nanotubes in an epoxy matrix and the resulting electrical properties”, *Polymer*, **40**(21), 5967-5971.
- Shams, S. and Soltani, B. (2015), “The effects of carbon nanotube waviness and aspect ratio on the buckling behavior of functionally graded nanocomposite plates using a meshfree method”, *Polym. Compos.*
- Shams, S. and Soltani, B. (2016), “Buckling of laminated carbon nanotube-reinforced composite plates on elastic foundations using a meshfree method”, *Arab. J. Sci. Eng.*, **41**(5), 1981-1993.
- Tagrara, S.H., Benachour, A., Bouiadjra, M.B. and Tounsi, A. (2015), “On bending, buckling and vibration responses of functionally graded carbon nanotube-reinforced composite beams”, *Steel Compos. Struct., Int. J.*, **19**(5), 1259-1277.
- Wattanasakulpong, N. and Chaikittiratana, A. (2015), “Exact solutions for static and dynamic analyses of carbon nanotube-reinforced composite plates with Pasternak elastic foundation”, *Appl. Math. Model.*, **39**(18), 5459-5472.
- Zhu, P., Lei, Z.X. and Liew, K.M. (2012), “Static and free vibration analyses of carbon nanotube-reinforced composite plates using finite element method with first order shear deformation plate theory”, *Compos. Struct.*, **94**(4), 1450-1460.

Appendix

With respect to Eq. (21) and Fig. 3, $\Pi^{(i)}$ ($i = 1, 2, 3$) are defined as

$$\Pi^{(1)} = \int_0^{\frac{d}{2}} \int_{-\frac{d}{2}}^{\frac{d}{2}} \left(\begin{aligned} & \mu^2 P \left(\frac{\partial^2 w^{(1)}}{\partial x^2} \right) + \mu^2 P \left(\frac{\partial^2 w^{(1)}}{\partial y \partial x} \right)^2 - \frac{1}{2} P \left(\frac{\partial w^{(1)}}{\partial x} \right)^2 + \mu^2 P \left(\frac{\partial w^{(1)}}{\partial x} \right) \left(\frac{\partial^2 w^{(1)}}{\partial x^3} \right) \\ & + \mu^2 P \left(\frac{\partial w^{(1)}}{\partial x} \right) \left(\frac{\partial^3 w^{(1)}}{\partial y^2 \partial x} \right) - 2\mu^2 K_w w^{(1)} \left(\frac{\partial^2 w^{(1)}}{\partial x^2} \right) + 2\mu^2 \left(\frac{\partial w^{(1)}}{\partial x} \right) G_p \left(\frac{\partial^3 w^{(1)}}{\partial y^3} \right) \\ & + 2\mu^2 \left(\frac{\partial w^{(1)}}{\partial x} \right) G_p \left(\frac{\partial^3 w^{(1)}}{\partial y^2 \partial x} \right) + 2\mu^2 G_p w^{(1)} \left(\frac{\partial^4 w^{(1)}}{\partial y^2 \partial x^2} \right) - 2\mu^2 K_w w^{(1)} \left(\frac{\partial^2 w^{(1)}}{\partial y^2} \right) \\ & + 2\mu^2 \left(\frac{\partial w^{(1)}}{\partial y} \right) G_p \left(\frac{\partial^3 w^{(1)}}{\partial y \partial x^2} \right) + 2\mu^2 \left(\frac{\partial w^{(1)}}{\partial y} \right) G_p \left(\frac{\partial^3 w^{(1)}}{\partial y^3} \right) + \mu^2 \left(\frac{\partial^2 w^{(1)}}{\partial y^2} \right)^2 G_p \\ & - w^{(1)} G_p \left(\frac{\partial^2 w^{(1)}}{\partial y^2} \right) + \mu^2 \left(\frac{\partial^2 w^{(1)}}{\partial x^2} \right)^2 G_p - 2\mu^2 K_w \left(\frac{\partial w^{(1)}}{\partial y} \right)^2 + K_w (w^{(1)})^2 \\ & + w^{(1)} G_p \left(\frac{\partial^2 w^{(1)}}{\partial x^2} \right) - 2\mu^2 K_w \left(\frac{\partial w^{(1)}}{\partial x} \right)^2 - \frac{1}{2} M_x \left(\frac{\partial^2 w^{(1)}}{\partial x^2} \right) \\ & - M_{xy} \left(\frac{\partial^2 w^{(1)}}{\partial y \partial x} \right) - \frac{1}{2} M_y \left(\frac{\partial^2 w^{(1)}}{\partial y^2} \right) \end{aligned} \right) dx dy, \quad (A1)$$

$$\Pi^{(2)} = \int_{\frac{d}{2}}^{\frac{d}{2}} \int_{\frac{d}{2}}^{\frac{d}{2}} \left(\begin{aligned}
 & \mu^2 P \left(\frac{\partial^2 w^{(2)}}{\partial x^2} \right) + \mu^2 P \left(\frac{\partial^2 w^{(2)}}{\partial y \partial x} \right)^2 - \frac{1}{2} P \left(\frac{\partial w^{(2)}}{\partial x} \right)^2 + \mu^2 P \left(\frac{\partial w^{(2)}}{\partial x} \right) \left(\frac{\partial^3 w^{(2)}}{\partial x^3} \right) \\
 & + 2\mu^2 K_w w^{(2)} \left(\frac{\partial^2 w^{(2)}}{\partial x^2} \right) + 2\mu^2 \left(\frac{\partial w^{(2)}}{\partial x} \right) G_p \left(\frac{\partial^3 w^{(2)}}{\partial x^3} \right) + \mu^2 G_p w^{(2)} \left(\frac{\partial^4 w^{(2)}}{\partial x^4} \right) \\
 & + 2\mu^2 \left(\frac{\partial w^{(2)}}{\partial x} \right) G_p \left(\frac{\partial^3 w^{(2)}}{\partial y^2 \partial x} \right) + 2\mu^2 G_p w^{(2)} \left(\frac{\partial^4 w^{(2)}}{\partial y^2 \partial x^2} \right) - 2\mu^2 K_w w^{(2)} \left(\frac{\partial^2 w^{(2)}}{\partial y^2} \right) \\
 & + 2\mu^2 \left(\frac{\partial w^{(2)}}{\partial y} \right) G_p \left(\frac{\partial^3 w^{(2)}}{\partial y \partial x^2} \right) + 2\mu^2 \left(\frac{\partial w^{(2)}}{\partial y} \right) G_p \left(\frac{\partial^3 w^{(2)}}{\partial y^3} \right) + \mu^2 \left(\frac{\partial^2 w^{(2)}}{\partial y^2} \right)^2 G_p \\
 & - w^{(2)} G_p \left(\frac{\partial^2 w^{(2)}}{\partial y^2} \right) + \mu^2 \left(\frac{\partial^2 w^{(2)}}{\partial x^2} \right)^2 G_p - 2\mu^2 K_w \left(\frac{\partial w^{(2)}}{\partial y} \right)^2 + K_w (w^{(2)})^2 \\
 & + 2\mu^2 \left(\frac{\partial^2 w^{(2)}}{\partial x^2} \right) G_p \left(\frac{\partial^2 w^{(2)}}{\partial y^2} \right) + \mu^2 P \left(\frac{\partial w^{(2)}}{\partial x} \right) \left(\frac{\partial^3 w^{(2)}}{\partial y^2 \partial x} \right) + \mu^2 w^{(2)} G_p \left(\frac{\partial^4 w^{(2)}}{\partial y^4} \right) \\
 & - 2\mu^2 K_w \left(\frac{\partial w^{(2)}}{\partial x} \right)^2 - w^{(2)} G_p \left(\frac{\partial^2 w^{(2)}}{\partial x^2} \right) - \frac{1}{2} M_x \left(\frac{\partial^2 w^{(2)}}{\partial x^2} \right) \\
 & - M_{xy} \left(\frac{\partial^2 w^{(2)}}{\partial y \partial x} \right) - \frac{1}{2} M_y \left(\frac{\partial^2 w^{(2)}}{\partial y^2} \right)
 \end{aligned} \right) dx dy, \quad (A2)$$

$$\Pi^{(3)} = \int_{-\frac{d}{2}}^{\frac{d}{2}} \int_0^{\frac{d}{2}} \left(\begin{aligned}
 & \mu^2 P \left(\frac{\partial^2 w^{(3)}}{\partial x^2} \right) + \mu^2 P \left(\frac{\partial^2 w^{(3)}}{\partial y \partial x} \right)^2 - \frac{1}{2} P \left(\frac{\partial w^{(3)}}{\partial x} \right)^2 + \mu^2 P \left(\frac{\partial w^{(3)}}{\partial x} \right) \left(\frac{\partial^3 w^{(3)}}{\partial x^3} \right) \\
 & + 2\mu^2 K_w w^{(3)} \left(\frac{\partial^2 w^{(3)}}{\partial x^2} \right) + 2\mu^2 \left(\frac{\partial w^{(3)}}{\partial x} \right) G_p \left(\frac{\partial^3 w^{(3)}}{\partial x^3} \right) + \mu^2 G_p w^{(3)} \left(\frac{\partial^4 w^{(3)}}{\partial x^4} \right) \\
 & + 2\mu^2 \left(\frac{\partial w^{(3)}}{\partial x} \right) G_p \left(\frac{\partial^3 w^{(3)}}{\partial y^2 \partial x} \right) + 2\mu^2 G_p w^{(3)} \left(\frac{\partial^4 w^{(3)}}{\partial y^2 \partial x^2} \right) - 2\mu^2 K_w w^{(3)} \left(\frac{\partial^2 w^{(3)}}{\partial y^2} \right) \\
 & + 2\mu^2 \left(\frac{\partial w^{(3)}}{\partial y} \right) G_p \left(\frac{\partial^3 w^{(3)}}{\partial y \partial x^2} \right) + 2\mu^2 \left(\frac{\partial w^{(3)}}{\partial y} \right) G_p \left(\frac{\partial^3 w^{(3)}}{\partial y^3} \right) + \mu^2 \left(\frac{\partial^2 w^{(3)}}{\partial y^2} \right)^2 G_p \\
 & - w^{(3)} G_p \left(\frac{\partial^2 w^{(3)}}{\partial y^2} \right) + \mu^2 \left(\frac{\partial^2 w^{(3)}}{\partial x^2} \right)^2 G_p - 2\mu^2 K_w \left(\frac{\partial w^{(3)}}{\partial y} \right)^2 + K_w \left(w^{(3)} \right)^2 \\
 & + \mu^2 P \left(\frac{\partial w^{(3)}}{\partial x} \right) \left(\frac{\partial^3 w^{(3)}}{\partial y^2 \partial x} \right) + 2\mu^2 \left(\frac{\partial^2 w^{(3)}}{\partial x^2} \right) G_p \left(\frac{\partial^2 w^{(3)}}{\partial y^2} \right) + \mu^2 w^{(3)} G_p \left(\frac{\partial^4 w^{(3)}}{\partial y^4} \right) \\
 & - 2\mu^2 K_w \left(\frac{\partial w^{(3)}}{\partial x} \right)^2 - w^{(3)} G_p \left(\frac{\partial^2 w^{(3)}}{\partial x^2} \right) - \frac{1}{2} M_x \left(\frac{\partial^2 w^{(3)}}{\partial x^2} \right) \\
 & - M_{xy} \left(\frac{\partial^2 w^{(3)}}{\partial y \partial x} \right) - \frac{1}{2} M_y \left(\frac{\partial^2 w^{(3)}}{\partial y^2} \right)
 \end{aligned} \right) dx dy, \quad (\text{A3})$$